Diatom-driven recolonization of microbial mat-dominated siliciclastic tidal flat sediments

Jerónimo Pan[a,b*], Diana G. Cuadrado[a,d,e], Constanza N. Bournod[a,d]

[a] *Consejo Nacional de Investigaciones Científicas y Técnicas (CONICET), Av. Rivadavia 1917, Buenos Aires (C1033AAJ), Argentina.*

[b] *Instituto de Investigaciones Marinas y Costeras (IIMyC, CONICET/UNMdP), Rodriguez Peña 4046, Mar del Plata (7600), Buenos Aires, Argentina*

[c] *Instituto de Geología de Costas y del Cuaternario (IGCyC, UNMdP/CIC), Funes 3350, Mar del Plata (7600), Buenos Aires, Argentina*

[d] *Instituto Argentino de Oceanografía (IADO, CONICET/UNS), Florida 7500, Bahía Blanca (8000), Buenos Aires, Argentina*

[e] *Departamento de Geología, Universidad Nacional del Sur, San Juan 670, Bahía Blanca (8000), Buenos Aires, Argentina.*

*corresponding author: jeronimopan@gmail.com, Phone: 54-9223-604-9812

Keywords: microbial mats, biological sediment colonization, ecological succession, microphytobenthos, filamentous cyanobacteria, diatoms

Manuscript submitted to: *FEMS Microbiology Ecology* (Prof. Max Häggblom, Editor-in-Chief), Patricia Sobecky (suggested Editor)

Submitted in revised form: 23-08-2017

ABSTRACT

Modern microbial mats and biofilms play a paramount role in sediment biostabilization. When sporadic storms affect tidal flats of Bahía Blanca Estuary, the underlying siliciclastic sediment is exposed by physical disruption of the mat, and in a few weeks' lapse, a microbial community re-establishes. With the objective of studying colonization patterns and the ecological succession of microorganisms at the scale of these erosional structures, these were experimentally-made and their biological recolonization followed for 8 wk, with replication in winter and spring. Motile pennate diatoms led the initial colonization following two distinct patterns: a dominance by *Cylindrotheca closterium* in winter; and by naviculoid and nitzschioid diatoms in spring. During the first 7 d, cell numbers increased 2-17-fold. Cell densities further increased exhibiting sigmoidal community growth, reaching 2.9-8.9 × 10^6 cells cm^{-3} maxima around d-30; centric diatoms maintained low densities throughout. In the 56 d after removal of the original mat, filamentous cyanobacteria that dominates mature mats did not establish a significant biomass, leading to the rejection of the hypothesis that cyanobacteria would drive the colonization. The observed dominance of pennate diatoms is attributed to extrinsic factors determined by tidal flooding; and intrinsic ones, e.g. motility, nutrient affinity, and high growth rate.

INTRODUCTION

Photosynthetic microbial mats are stratified consortia of prokaryotes and eukaryotes, initially developed as biofilms at sediment-water interfaces in shallow and intertidal marine sediments, corresponding to the oldest, most widespread evidence of early life on Earth (Des Marais 2003). The driving force of microbial mats is photosynthesis by cyanobacteria and eukaryotic microalgae (van Gemerden 1993; Stolz 2000). Filamentous cyanobacteria form laminated multilayers that are covered by layers of eukaryotic diatoms (e.g. *Navicula* spp., *Nitzschia* spp., *Amphora* spp.) embedded in exopolysaccharides excreted by the benthic microbial community (Cohen and Gurevitz 2006) conferring stability to sediments. Microbial mats are complete, self-sufficient ecosystems that recycle nutrients and play a paramount role in sediment biostabilization in present-day tidal flats. The properties and behavior of intertidal marine sediments cannot be understood without taking their phototrophic microorganisms into account; thus microphytobenthos (MPB) has been recognized as a biogeomorphological force (reviewed by Stal 2010).

Much attention has been paid to the seasonal variation in microbial communities of estuarine sediments, largely focusing on species dominance, chlorophyll-*a* content (a proxy for microphytobenthic biomass), extracellular polymeric substances (EPS) production, and the correlation of all these factors with sediment stability (Admiraal et al. 1984; Underwood and Paterson 1993; de Jonge and Colijn 1994; Underwood 1994). Researchers have also focused on seasonal *biofilm development*, within microbial communities dominated by either cyanobacteria (Noffke and Krumbein 1999) or by epipelic diatoms (Scholz and Liebezeit 2012).

However, there is a distinction to be made between seasonal succession of different taxa, ecological groups or physiologic guilds of microorganisms, and the *ecological succession* of microorganisms that colonize naturally- or artificially-disturbed sediment substrates. Ecological succession, the self-organizational process by which ecosystems develop structure and functions from available energy sources (Odum 1983), not only shapes biological communities, but can also have profound effects in the transformation of the physical medium in which biotic agents grow and develop. A periodic return to start-up conditions might take place spontaneously in some ecological systems, or what Odum (1971) considers a "pulsing system with continual restart", in which "the energy accumulated in succession may be used to undo its own work".

Filamentous cyanobacteria have been recognized as the most successful components in the succession and enlargement of a biofilm community into a microbial mat (Gerdes 2007); they are also pointed as the dominant community component in mats from most shallow marine and hypersaline environments (Des Marais 2003; Cohen and Gurevitz 2006). The cosmopolitan filamentous cyanobacterium, *Microcoleus chthonoplastes*, is recognized as the species dominating in biomass and structuring microbial mats worldwide, and also for our study site, the Bahía Blanca Estuary in Argentina (Parodi and Barría de Cao 2003; Pan et al. 2013*a*; *b*). Sporadic storms affect microbial mats in the lower supratidal of Bahía Blanca Estuary (Cuadrado et al. 2011; 2013) forming structures such as erosional pockets (*sensu* Noffke 1999) and flipped-over mats (*sensu* Schieber 1999). The underlying denuded sediments then get recolonized after a few wk by a new microbial community, ultimately leveling the erosional structure with the rest of the supratidal flat. Accordingly, this paper originated in the hypothesis that a physical disruption of the mat would trigger a biological response, in which filamentous cyanobacteria (i.e. the dominant component of mature mats) would lead the recolonization. Therefore, the objective of this study was to experimentally study the colonization pattern and the ecological succession of microorganisms in the field, at the scale determined by the erosional structures that occur naturally. In order to evaluate this, the approach of this paper was to create analogous erosional structures and follow their recolonization by progressive sampling under natural conditions. To our knowledge, this *in situ* experiment is the first of its kind, providing "real-world" data of the succession in a complex system, such as a microbial mat.

METHODS

Location and experimental design

Field experiments were carried out in the lower supratidal zone of Puerto Rosales (38º 55´ S; 62º 03´ W), on central Bahía Blanca Estuary (Argentina), where extensive tidal flats (~ 1000 m wide) with low slopes (~ 0.4º gradient) are composed of muddy to sandy siliciclastic sediments (Fig. 1A). The presence of *Spartina alterniflora* in the intertidal zone attenuates wave action, dissipating the hydraulic energy and absorbing wave energy (Koch et al. 2009), thus reducing the capability of currents to erode and transport sediments (Wolanski et al. 2009). This vegetation shield protects the study site from erosion, promoting a low sedimentation rate and favoring the colonization by MPB communities that form biofilms and microbial mats (Cuadrado et al. 2011; Pan et al. 2013*b*). Sediments are mostly azoic, except for patches colonized by the crab *Neohelice granulata*.

Experiments were replicated in Austral winter (Julian days 151-207) and late spring (Julian days 280-357) in order to contrast seasonal influences over the colonization process, at two experimental sites described at length in Cuadrado et al. (2011) (namely, Sites 1 and 3); which are referred to as **S1W** and **S3W** for winter, and **S1S** and **S3S** for spring, respectively. A previous study by Pan et al. (2013a) at the same sites as

this study, focused on the physical parameters (solar radiation and sediment temperature at -5 cm) and the effect that these have on microbial mats. An inverse relationship between microphytobenthic abundance and sediment temperature and solar radiation was found with linear regressions, but this has a strong seasonal component. Tidal height data were obtained from a tidal gauge at Puerto Belgrano located 4 km from the study area toward the inner portion of the estuary (Fig. 1A). The minimum tidal height needed for seawater to flood the supratidal zone varies according to topographic differences in height between the sites (Cuadrado et al. 2013); this height was estimated empirically during this study as ≥ 3.98 m for Site 1, and ≥ 4.18 m for Site 3. Wave height in conjunction with wind parameters (speed and direction) were measured at the Oceanographic Tower in the estuary entrance.

At each site, the surface microbial mat and underlying siliciclastic sediments (topmost ~ 2 cm) were removed delimiting a 225 cm^2 square area; the choice of square (15 × 15 cm) experimental patches attended to the "polygonal" shape of naturally-occurring sedimentary structures (i.e. erosional pockets, flipped-over mats) with comparable surface area at the study site. In turn, these experimental quadrats were subdivided into 84 regularly-spaced sampling points, separated ~ 1.66 cm from each other. Sampling consisted in taking sediment cores (polypropylene, cylindrical: 0.385 cm^2 area, ~ 0.3 cm height) twice every wk (every 3 or 4 d) for 6 wk following removal of the original sediment/biofilm layer, and then every 7 d for another 2 wk (Fig. 1B). On any sampling event, n = 6 samples were taken randomly across the sampling quadrat, so that at the end of the experimental period all points were sampled a single time. Sampling was consistently done during daytime and at low tide.

Additionally, sediment cores were taken mid-point and at the end of each experiment, on adjacent (~ 50 cm) control patches of undisturbed microbial mat, in order to monitor natural shifts in the density and composition of the microorganisms at each experimental site.

Sample processing

Sediment cores were preserved in 5 % acidic Lugol's iodine solution (stock solution prepared with natural filtered seawater), and re-suspended into 50 ml. In order to disassemble the mat fabric and enhance contact of the preservative with the microorganisms, samples were homogenized in a shaker (Bandelin Sonorex Tk52). 1-ml aliquots were taken from the resuspension and microorganisms were enumerated using a Sedgewick-Rafter chamber (LeGresley and McDermott 2010) with a Nikon YS2-T compound microscope. Cyanobacteria and diatoms were identified to the lowest possible taxonomic level; the identification of cyanobacteria was based on Waterbury (2006), while, the analysis of diatoms followed a size-class and taxonomic criterion (Round et al. 1990). Wunsam et al. (2002) concluded that size distribution and coarse (genus level) taxonomic analyses sometimes outperformed fine taxonomy in describing the response of diatom assemblages to environmental stimuli.

Floristic comparisons between the pennate and centric diatoms were done by converting densities to biomass (biovolume) estimates. Biovolume was estimated from linear cell dimensions of representative genera of pennate and centric diatoms (a minimum of n = 15 cells were measured for each) applying geometric models (Sun and Liu 2003). Then a biomass ratio was calculated between pennate:centric diatoms. Mean values ± SE, were calculated from the biomass data on n = 6 randomly-distributed points in the plot, for each date.

Graphic plots

Graphic plots were produced with the surface- and contour-mapping program Surfer v.10 (Golden Software, Inc.), and using the minimum curvature as gridding method. The number of lines to construct the grid geometry was 9 × 9 to coincide with the sample position. Each sampling point was referenced to the experimental 15 × 15 cm quadrat, into which total cell densities were input, considering three lapses (0-14; 18-32 and 35-56 d), comprising the total length of the experiment. Thus, a set of three spatially-adjusted two-dimensional plots that integrate the spatial aggregation of microorganisms at three time intervals were produced for each experimental run.

Statistical analysis

Differences in diatom and cyanobacteria cell densities were tested by means of a two-factor ANOVA with replication, with sampling date and taxonomic group as factors. The same was applied to test for differences between densities of pennate and centric diatoms, with sampling

date and diatom group as factors. For each experiment, the null hypothesis of no differences in cell densities between sampling dates was evaluated by means of single-factor ANOVA. Comparisons of cell densities between experimental plots and undisrupted control patches were made by single-factor ANOVA (Zar 1999).

RESULTS

There were significant differences in cell density between control- and experimental plots, at the middle and end of experimental runs at both sites (Table 1). After the onset of the recolonization, all experimental plots showed significantly higher cell densities than the adjacent undisturbed microbial mat; these densities corresponded mostly to diatoms. These differences ranged from a 7.2-fold and 9.5-fold greater cell density at day 28, for **S1W** and **S3W**, respectively; to a 36.3-fold difference at day 56 in **S3W**, and 63.1-fold larger cell density midway through **S1S**.

The stepwise, successional colonization of all denuded experimental plots was evidenced by statistically-significant differences in total cell densities between sampling dates [single-factor ANOVA: **S1W**, $F(13, 70) = 12.3$, $p < 0.001$; Fig. 2A line. **S3W**, $F(13, 70) = 10.5$, $p < 0.001$; Fig. 2B line. **S1S**, $F(13, 70) = 13.6$, $p < 0.001$; Fig. 2C line. **S3S**, $F(13, 70) = 4.9$, $p < 0.001$; Fig. 2D line]. Diatoms were responsible for a steady colonization of the experimental quadrats, which, averaging total cell counts, exhibited sigmoidal community growth curves characteristic of many diatoms (Eppley 1977), at least during some time interval. An exception to this was **S3S**, which exhibited several exponential pulses of community growth (Fig. 2D). Raphid pennates e.g. *Cylindrotheca closterium*, *Navicula gregaria, Navicula phyllepta* and *Nitzschia palea* were present at, and became dominant from the onset of the recolonization; as an example, this is presented in Fig. 3. Towards the end of experiments these colonist taxa were still present, and at higher densities. In general, the maximum density of pennate and centric diatoms was reached at a time interval between days 24-35, followed by a decline in the following days.

Worth mentioning, is the fact that the dispersion of data for each date got progressively larger (see standard error bars in Fig. 2), as the recolonization progressed. This is to be expected, provided each point is an average of n = 6 cell density values, obtained from random sampling points across experimental quadrats. On average, cell densities were greater in experimental plots at Site 1 (2.9×10^6 cells cm^{-3}) than at Site 3 (1.8×10^6 cells cm^{-3}).

For all experiments, cell densities of pennate and centric diatoms were significantly different [two-factor ANOVA with replication: **S1W**, sampling date: $F(13, 140) = 11.8$, $p < 0.001$; diatom group: $F(1, 140) = 306.4$, $p < 0.001$; Fig. 2A bars. **S3W**, date: $F(13, 140) = 10.4$, $p < 0.001$; group: $F(1, 140) = 219.2$, $p < 0.001$; Fig. 2B bars. **S1S**, date: $F(13, 140) = 13.2$, $p < 0.001$; group: $F(1, 140) = 361.5$, $p < 0.001$; Fig. 2C bars. **S3S**, date: $F(13, 140) = 4.9$, $p < 0.001$; group: $F(1, 140) = 106.4$, $p < 0.001$; Fig. 2D bars]. Thus, the two groups of diatoms exhibited distinct colonization patterns. Pennate diatoms dominated numerically the MPB community at both study sites (Fig. 2), with the exception of the initial conditions for three out of four experimental runs (Figs. 2A, B, D). Pennates were also dominant in terms of biomass (Table 2), with the sole exception of the first wk after the removal of the microbial mat in **S1W**, in which the biomass of centric diatoms was ~ 50 % greater than that of pennates. The latter was due to a dominance of chain-forming centrics, e.g. *Melosira* sp., *Paralia sulcata*, *Podosira* sp., during the first 3 d.

An analysis of the pennate:centric biomass ratio (Table 2), points that the biomass of pennate diatoms was not only dominant from the onset, but it also built up as the recolonization progressed, as it is evidenced by the progressive increment in the ratio. For instance, in the winter experimental runs, there was a 13.5-fold and 3.2-fold increment in the ratio, between day 0 and day 56, for **S1W** and **S3W**, respectively. While centric diatoms sustained stable populations with little variation in cell densities (increasing densities up to 7.2-fold in **S1S**, and peaking at ~ 0.4 $\times 10^6$ cells cm^{-3}), pennate diatoms presented higher variability. The relative contribution of centric diatoms to the total cell density decreased with the density increment of pennates as the recolonization progressed. Conversely, when total cell numbers were low (e.g. at the beginning of experiments **S3W** and **S3S**; Figs. 2B, D), or when cell densities decreased significantly (e.g. day 42 for **S3S**; Fig. 2D), the proportion of centric diatoms in the community was > 40 %.

There were two distinct patterns of early colonization among raphid pennate diatoms. During winter experiments, the needle-like *C. closterium* was the pioneering species that quickly became numerically dominant and remained such during the time lapse that the experiments lasted (Figs. 3A, 3B). In these cases, *C. closterium* presented the highest cell densities of all diatoms, peaking at 3.1 $\times 10^6$ cells cm^{-3} in **S1W**, with a 18.9-fold population increment on day 42 (Fig. 3A). With these spikes in cell density (e.g. on days 7, 31 and 35 in **S1W**, Fig. 2A; and days 24, 28 and 56 in **S3W**, Fig. 2B), *C. closterium* not only contributed the most of all species to total cell density variations, but also influenced the pattern for total cell density at large. Even at their maximum density (~ 0.9 $\times 10^6$ cells cm^{-3} on day 50 in experiment **S1W**), and despite steady density increments on both winter experiments, naviculoid pennates remained at much lower densities than *C. closterium*. However, it should be considered that in terms of biomass, naviculoid pennates have ~ 5× the biovolume of *C. closterium*, when geometric models (Sun and Liu 2003) are applied.

Conversely, during the spring experiments, the pioneering community was composed of small (mean apical axis = 24.0 µm; mean transapical axis 7.5 µm; n = 22) naviculoid and nitzschioid pennates (namely, *N. gregaria*, *N. phyllepta*, and *N. palea*). Once established from the onset, this *Navicula*-dominated recolonization produced cell densities that at times were two-to-three orders of magnitude higher than that of any other diatom (Figs. 3C, D). Moreover, at 8.7 $\times 10^6$ cells cm^{-3} on day 32 of **S1S**, naviculoid and nitzschioid pennates yielded the highest densities of all experiments. In experiment **S3S** *C. closterium* presented density variations that closely followed those of naviculoids and nitzschioids (Fig. 3D); however the pattern of cell density variations reversed, from day 49-56, when a 3.7-fold increment in naviculoids corresponded simultaneously with a 36 % reduction in *C. closterium* densities.

These inversed trends in *C. closterium* and naviculoid densities were also common in later stages of other experiments. For instance, in **S1S** from day 25-32, there was a 10-fold decrement in *C. closterium*, correlating with a 2.9-fold increment in naviculoids. After that, from day 32-35 naviculoids decreased 5.5-fold, while *C. closterium* increased 2.3-fold (Fig. 3C). Likewise, from day 35-42 of **S1W**, there was a 1.2-fold increment in the cell density of *C. closterium*, together with a 39 % decrement in naviculoids; from day 42-50, *C. closterium* decreased 40 % coinciding with a 2.2-fold increment in naviculoids; finally, in the 50-56 d time lapse, *C. closterium* increased 1.6-fold, while naviculoids and nitzschioids decreased their density by 47 % (Fig. 3A).

Not only were there progressive changes in cell densities, but also "successional" changes involving the alternation of different taxa. A frequent pattern included the presence of a few cells of large (> 120 µm) pennate diatoms such as *Gyrosigma spencerii* and some large (> 65 µm) individual centric diatoms such as *Coscinodiscus* sp. and *Actinocyclus* sp. right after the removal of the microbial mat. Likewise, cyanobacteria trichomes (mostly *M. chthonoplastes*) were more frequently found on initial dates. Further into the colonization, larger raphid pennates (e.g. *Amphora ovalis*, *Amphiprora* sp., *Rhopalodia* sp., *Diploneis* sp.) with individual cells that on average have ~ 10 × the biovolume of pre-established naviculoid and 'nitzchioid' pennates, were represented in the community. These larger, more robust pennates, appeared together with < 50 µm solitary- and chain-forming (~ 20 µm in length) centric diatoms (e.g. *Paralia sulcata*, *Melosira* sp., *Podosira* sp.). From the fourth wk into the recolonization onwards, the population densities of these taxa started to shift, making it difficult to establish a distinct succession pattern.

The cell densities of the three major groups of microorganisms (i.e. filamentous cyanobacteria, pennate and centric diatoms) were significantly different in all experimental runs [two-factor ANOVA with replication: **S1W**, sampling date: $F(13, 210) = 11.8$, $p < 0.001$; taxa: $F(2, 210) = 343.6$, $p < 0.001$; Fig. 2A bars. **S3W**, date: $F(13, 210) = 10.5$, $p < 0.001$; taxa: $F(2, 210) = 259.9$, $p < 0.001$; Fig. 2B bars. **S1S**, date: $F(13, 210) = 13.2$, $p < 0.001$; taxa: $F(2, 210) = 382.5$, $p < 0.001$; Fig. 2C bars. **S3S**, date: $F(13, 210) = 4.8$, $p < 0.001$; taxa: $F(2, 210) = 149.0$, $p < 0.001$; Fig. 2D bars]. The density of cyanobacterial trichomes and their biomass were significantly lower in relation to diatoms. As above-mentioned, *M. chthonoplastes* appeared either right after or during the first wk following the removal of the microbial mat, in three of the experimental surveys (**S1W**, **S3W** and **S3S**). In three of the experiments it was found again only on later dates (i.e. at day 24 in **S3W**; at day 32 in **S1S**; and at days 49 and 56 in **S3S**). Other filamentous cyanobacteria (*Oscillatoria limosa* and *Arthrospira* sp.) were found right after the

removal or during the first wk of recolonization (at both experiments in Site 3), and they usually took much longer than diatoms to colonize the denuded sediment in **S1S**, appearing only on day 42 and 49. *O. limosa* and *Arthrospira* sp. were found more frequently at Site 3, where they were sampled on eleven out of the fourteen sampling events. Nearly 40 % of the points on which filamentous cyanobacteria were sampled, were located on the margins of the experimental patch (see border effect below). However, the average density of non-heterocystous filamentous cyanobacteria remained low throughout the experiment (peaking at 3.7×10^4 trichomes cm^{-3} in Site 3), appearing sporadically in most samples.

Regarding the spatial progression of the recolonization in experimental plots, the contribution of borders to the development of a microbial community was evidenced in the first wk (0-14 d after removal of the mature microbial mat), as it is shown in the left plots in Fig. 4. The recolonization in **S1W**, progressed from a "focal" spot with a density > 4.0×10^6 cells cm^{-3} on the left and upper borders, that were still present at intermediate times (17-31 d after removal), and rearrange into a mosaic of higher densities (> 4.5×10^6 cells cm^{-3}) by the time interval of 35-56 d, with two distinctive peaks in the center of the plot, and three more distributed on the two upper corners, and lower border (Fig. 4A). Sharp gradients arise between high- and low-density areas, determining a mosaic-type aggregation of MPB (clearly seen in Fig. 4A right; also in Figs. 4B right; 4C middle; 4D middle). The recolonization of the plot in **S3W** was more moderate than that in Site 1, with a few high cell density spots (~ 3.0×10^6 cells cm^{-3}) arising in the lower right and left corners by days 17-31, to later rearrange into two distinct high density spots (~ 5.0×10^6 cells cm^{-3}) by days 35-56, localized on the lower right and central zones of the plot (Fig. 4B). The plot in **S1S** presented the highest densities (~ 9.0×10^6 cells cm^{-3}) in the time interval of 18-32 d, shown in the center graph in Fig. 4C as a "spike" penetrating from the top towards the center of the plot, which evolved from a moderate concentration of cells (~ 3.0×10^6 cells cm^{-3}) in the upper border on the previous time interval (0-14 d). The pattern then got diffused into a mosaic of high-density (~ 6.0×10^6 cells cm^{-3}) spots, by days 35-56. The plot in **S3S** got recolonized from the left border towards the center. By the 18-32 d time interval a few diffuse spots with high cell density (> 4.0×10^6 cells cm^{-3}) appeared, corresponding to the peaks in cell density at days 18 (upper left) and 32 (center and upper border) in Fig. 2D. Despite a steep fall in cell densities after day 32, these high-density spots evolve into a "spike" (~ 3.0×10^6 cells cm^{-3}) running towards the center of the plot from the upper left corner.

A photographic sequence of the experimental plots (Fig. 5), brings into evidence some processes taking place in the supratidal flat. The contrast in appearance between winter and spring at both sites, points to the marked difference between seasons in tidal re-wetting of the plots. The two sites present topographic differences and get flooded differentially; accordingly, during the winter experiments, Site 1 was regularly flooded 56 times over the 56 days that the experiment lasted (Fig. 3A1); the peaks in density of *C. closterium* and naviculoids at day 7, and after the first 28 d, coincide with previous periods of continuous re-wetting of the site. On the other hand, Site 3 was flooded only 21 times during the winter experiment, experiencing frequent flooding during the first 5 d, and then in the days 21-28 time lapse (Fig. 3B1); as in Site 1, the steady density increment of *C. closterium* and naviculoids from day 21 onwards, coincides with frequent re-wetting of the supratidal pan.

On the other hand, the pattern for spring evidenced regular flooding of Site 1, reaching maximum water height around day 28 (Fig. 3C1) providing optimal conditions for naviculoids to peak at day 32; while Site 3 experienced 18 sporadic flooding events, mostly from day 32 onwards (Fig. 3D1). Despite not having tidal height records for the days 28-32 time lapse in **S3S**, the filling with sediment of sampling points during those two consecutive sampling dates (Fig. 5), indicates that the site was flooded; this correlates with a spike in cell densities of naviculoids and *C. closterium* from days 25-32. From Fig. 3D1, it is clear that **S3S** was the experimental plot least influenced by tidal wetting, and accordingly the desiccation cracks that were present at the beginning of this experiment remained throughout the survey period, which points to an elevated rate of evaporation (Fig. 5). The tidal inundation causes a re-distribution of sediments and leveling of the experimental patches which was more marked in spring at both sites (Fig. 5). In turn, this larger input of sediments might have accounted for a "dilution effect", lowering the cells densities.

DISCUSSION

The experiments in this study showed a clear dominance of pennate diatoms, acting as pioneers in the colonization of denuded sediments devoid of accumulated organic matter, in which the vertical physico-chemical fluxes were drastically modified by the experimental setup. Thus, the hypothesis that the filamentous cyanobacteria that dominate mature mats would drive the recolonization following a physical disruption is rejected.

The ability of benthic pennate diatoms to colonize adverse environments, has been linked to their capacity to withstand darkness and thrive in anoxic and sulfide-rich sediments (Kennett and Hargraves 1985; Kamp et al. 2011), in which cases EPS production might act as a buffering mechanism against a harsh chemical milieu (Decho 1990). On the other hand, marine diatoms have acquired over the course of their evolution, a genetic plasticity (Bowler et al. 2010) to exert a competitive advantage over other colonizers, and are usually the first group to exploit resources and dominate, both in the plankton and the benthos.

In ecological succession, the smallest components with rapid turnovers are the ones to first colonize the substratum (Odum 1983). With their ability to rapidly colonize physically-disturbed sediments, small-sized diatoms outcompete larger, slow-growing cells. This competitive advantage undoubtedly lies in their high growth rate; smaller cells are more active due to their larger surface:volume ratio, having higher growth- (Williams 1964), photoshynthetic-, and nutrient-absorption rates (Snoeijs et al. 2002). One of the outcomes of this study was that in winter *C. closterium* dominated the recolonization from the onset. *C. closterium* has a much higher growth rate than many other diatom species (Tanaka 1984) estimated at > 2.3 doublings per day in culture (Kingston 2009), and it also exhibits the typical gliding motion of pennate diatoms (Edgar and Pickett-Heaps 1984; Apoya-Horton et al. 2006). On the other hand, small naviculoid and nitzschioid raphid diatoms took over first during spring. This had been previously noted by Pizani (2008) at this location, who pointed *N. phyllepta* and other naviculoids as early colonists after dredging works. Likewise, Morin et al. (2007) mention the monoraphid species *N. palea* and *N. gregaria* as well-represented species in their colonization experiments. The dominance of small species of the genus *Navicula* is also a common feature in intertidal flats of many estuaries, such as Marennes-Oléron (Haubois et al. 2005), Ems-Dollard, (Admiraal 1984), Severn (Underwood 1994), and Colne (Underwood et al. 1998).

The colonization of a sedimentary substrate not only brings changes to its biological identity, but also alters its biogeochemical properties of the sediment through numerous mechanisms, the most immediate one of which is the secretion of EPS, a product of phytosynthesis. Fernández et al. (2016) studied the seasonal and spatial dynamics of colloidal and capsular extracellular carbohydrates at the same site of our study and found that the colloidal carbohydrate fraction was predominant in surface sediments (0-5 mm), while the capsular fraction was predominant in subsurface layers (5-10 mm). Moreover, the maximum concentration of extracellular carbohydrates coincided with the annual peak in chlorophyll-*a*, pointing to a larger contribution of the colloidal fraction actively secreted by MPB, rather than the capsular, more recalcitrant, fraction.

In this study, we documented opposing, alternating cell density increments or decrements for *C. closterium* and naviculoids, regardless of the taxon that dominated the recolonization process. de Jong and Admiraal (1984) experimentally cultured three species of intertidal diatoms (*Navicula salinarum*, *C. closterium* and *Amphiprora* cf. *paludosa*) in unialgal- and mixed cultures, and found that the abundance of a certain species in mixed cultures was primarily determined by their capacity to produce inhibitory substances. However, contrary to the pattern described for our experiments, in mixed incubations of *N. salinarum* and *C. closterium*, these authors found that the former dominated at lower temperatures (8°C and 12°C), while the later dominated at 20°C. Also, as a strategy during interaction with a competitor, a certain species narrowed considerably the range of physico-chemical conditions it exploited. Du et al. (2012), studied differential photosynthetic responses in relation to vertical migration, considering the morphological characteristics of either cell type. *C. closterium* has long, narrow and only lightly or partially silicified valves so it can move more quickly through sediments by rotating their frustules (twice as fast as the shorter-valved *Nitzschia* sp.) Therefore, these authors concluded that motile benthic diatoms exhibit species-specific responses to light and temperature due to differences

in photosynthetic capability and morphological characteristics. In sum, the alternating shifts in densities of naviculoids and *C. closterium*, might have been related to a fine-tuning in resource (nutrient, light) utilization by either taxa and their autoecology.

Only a few studies have paid attention to diatom species interactions in MPB community development; one such study (Mitbavkar and Anil 2007) followed the establishment and progression of diatom fouling communities, at different nutrient loads. These authors found that an abundance of nutrients favored species with comparatively higher growth rates, thereby suppressing the growth of other co-existing species; fast immigrants that settled earlier were then replaced by fast reproducers; also, the initial density of the inoculum plays an important role in interspecific competition. This is particularly relevant, considering the alternative pathways of density-dominance followed by a *C. closterium*-dominated recolonization in winter *versus* a naviculoid-dominated colonization in spring.

Early in succession, the increment in biomass is one of the products of the net production (Odum 1983). Accordingly, Hillebrand and Sommer (2000) studied the response of estuarine microalgal diversity to colonization time over a 12-wk period and described a pattern with dominance of a few species, and a greater importance of algal growth on the substrata compared to the arrival of new species. Even if the continual replacement is a major source of stability, especially for scarce members, if the initial state is underseeded with species, its diversity may increase in later stages (Odum 1983).

Competitive, diversified systems produced by stable environmental conditions, such as microbial mats (van Gemerden 1993; Des Marais 2003), have high levels of accumulated biomass that are being constantly recycled (Odum 1971). In the face of a disruption, successional invaders make use of the energy source that sustain the system (in this case, nutrients), but are apt enough to thrive in an energy-impoverished system that lacks the complex, diverse structure and stabilized chemical cycles which were previously gained over stable conditions. Underwood and Barnett (2006) emphasized the role of nutrients as a strong environmental variable influencing species composition; for instance, Pringle and Bowers (1984) found that the addition of phosphate enhanced diatom growth in species of the genus *Navicula* and *Nitzschia*. In the study area, pore-water nutrients were independently monitored for June and July (i.e. the first experimental run in this study) at both sites, by Spetter et al. (2015). On average, these authors found higher DIN (dissolved inorganic nitrogen) concentrations at Site 1 (46.88 μM) than at Site 3 (25.15 μM); and the same was true for phosphate (Site 1 = 81.76 μM; Site 3 = 63.22 μM); whereas the averaged silicate concentrations were higher in the pore-water of Site 3 (239.31 μM), than at Site 1 (158.42 μM). From these concentration ranges, it is clear that there would be no nutrient limitation under normal circumstances for the community growth of MPB and the development of microbial mats.

On the other hand, primary production by diatom MPB rapidly sequesters the re-mineralized nutrients in pore-water (Sundbäck et al. 1991; Webster et al. 2002). In that regard, a small cellular size, which implies a high surface:volume ratio, provides a competitive advantage in nutrient-impoverished systems. The removal of the microbial mat may have affected the vertical flux of pore-water nutrients, impoverishing the nutrients in the topmost sediment, and promoting the differential development of populations of "colonialists" with lower nutrient requirements. In fact, the slender *C. closterium* and small naviculoid and nitzschioid pennate diatoms were the first ones to colonize the sediment.

Even when filamentous cyanobacteria in the genus *Oscillatoria* have been pointed as pioneering colonists (Stal et al. 1985; Noffke and Krumbein 1999; Gerdes et al. 2000), they appeared only at Site 3 in early stages of the recolonization; and only in later stages (days 42 and 49) of the **S1S** experiment. Likewise, *M. chthonoplastes*, only seems to have settled for colonization of the experimental quadrat in **S3S**, from day 49 onwards despite being pointed as indicative of mature mats (Stal et al. 1985; van Gemerden 1993; Noffke 1998; Stolz 2000). It is apparent that the time over which the experimental plots were monitored, did not suffice for filamentous cyanobacteria to establish stable, and dominant populations. Conversely, Noffke (1998) described alternative colonization patterns dominated either by filamentous cyanobacteria (*M. chthonoplastes*, *O. limosa*), or coccoid forms (*Merismopedia punctata*) in the lower supratidal of the North Sea. Despite the key role played by trichome motility (such as the gliding movement exhibited by *M. chthonoplastes*; Whale and Walsby 1984) in filament aggregation and the creation of a reticulate fabric (Shepard and Sumner 2010), filamentous cyanobacteria in our study fell short to pennate diatoms in the

colonization of denuded sediments. Odum (1971) emphasizes on a certain period required to build up the energy storages, pass through the life cycle of colonizers, clear competitors and set nutrient regeneration in motion. This period ultimately determines the timing for a return to mature conditions, which was not attained during the time lapse that our experiments lasted.

Anthropic disturbance caused by activities such as dredging may favor a diatom-dominated MPB community over a cyanobacteria-dominated one (Parodi and Barría de Cao 2003). Pizani et al. (2006) found that hydraulic dredging triggered a quick population response by pennate diatoms, which recolonized this tidal flat. In fact, on this section of the Bahía Blanca Estuary, typically laminated mats consist of a thick light-attenuating diatom biofilm developing over a mesh-like fabric of filamentous cyanobacteria. Diatoms present a vast array of regulatory physiological photoprotective mechanisms (Barnett et al. 2015) and may outperform cyanobacteria at high solar irradiances (Kruschel and Castenholz 1998). Thus, the failure of filamentous cyanobacteria to establish a critical biomass in the experimental plots might lie in the absence of this form of "biological shading" (Margulis and Dolan 2002) by lacking a thick-enough diatom biofilm at the onset of the recolonization. This suggests that colonization by cyanobacteria in this tidal flat may be compromised during the initial stages, until a thick diatom biofilm capable of attenuating solar radiation develops.

We observed a marked tendency for border effects in the spatial analysis of the recolonization process. In most experimental runs, regardless of seasonality, colonizing species started "intruding" the quadrat from multiple focal points at the borders, which vary in number, cell density and composition according to the marginal remaining populations of microorganisms (Paterson 1994). Species that dominate early stages tend to immigrate quickly (Stevenson et al. 1991). Having chosen a square shape, might have promoted the appearance of border effects; however, as previously pointed, our choice of such shape was not arbitrary, but rather based on the polygonal shapes that form naturally in the supratidal flat due to storm events (Cuadrado et al. 2011; see Fig. 10a in Cuadrado et al. 2014). Likewise, Seuront and Spilmont (2002) based their study of spatial aggregation of MPB, in 100 × 100 cm square quadrats, and they also found border effects (see Fig. 5 in Seuront and Spilmont 2002). The density increments in the MPB community were evidenced by high-density spots, which indicates that the growth of the biofilm was localized and heterogeneous, determining a mosaic-type aggregation of cells, creating sharp gradients occurring between high- and low-density areas at a microscale (< 1m; Figs. 4A right; 4B right; 4C middle; see also Fig. 8 in Seuront and Spilmont 2002). The spatial distribution of MPB revealed a high degree of heterogeneity, resulting from endogenous processes (e.g. reproduction, migration and death), and exogenous ones (tides, nutrient and sediment), that ultimately determine the significant biomass.

Physical processes such as tidal inundation and sediment transport, play a significant role throughout the recolonization, regulating biological aspects, such as biomass gain, and physical ones, such as sedimentary filling and the evening-out of surface "topographic" differences. The drastic fluctuations in cell densities observed mostly in the spring experiments (Figs. 2C, 2D; 3C, 3D) might be closely related to periods of desiccation and re-wetting of the supratidal flat due to tidal flooding (Figs. 3 and 5). These periods were variable, usually lasting between 3 and 9 d at a time. The vertical migration of pennate diatoms into deeper, more humid sediment layers during dry periods, is the behavioral strategy that this dominant group takes to avoid death by desiccation (McKew et al. 2011) and elevated salinity (Sauer et al. 2002; Apoya-Horton et al. 2006), and prevent temperature and radiative stress (Underwood 2002). A large proportion of the migrating diatoms remain biologically viable in the dried sediment, which enables a rapid recovery when the supratidal flat gets flooded, hence vertical migration is an important mechanism for the persistence of populations (Consalvey et al. 2004). On the other hand, the shifts in numerical dominance among different groups of diatoms can be explained by autecological differences in their nutrient niches (Underwood and Provot 2000), or by interspecific competition for nutrients, which can become more important than competition for light (Stevenson et al. 1991). The role of resuspension of cells and sedimentary particles and their horizontal redistribution at the boundary layer should also be considered. MPB is constantly transported and redistributed by tidal currents (Riznyk and Phinney 1972). Stevenson (1983) demonstrated that currents not only transport diatoms *per se*, but also have an impact in the rate of diatom migration. This author demonstrated empirically that the accumulation of diatoms on substrates (a proxy for diatom

community development) changes microhabitat characteristics, and this, in turn is modulated by the intensity of currents. This is particularly relevant for our study, provided the supratidal flat did not inundate frequently, and profound changes in community composition and macroscopic structure were observed after tidal inundation of the experimental plots.

It is known that for unicellular organisms that live at very low Reynold's numbers (i.e. when viscous forces prevail over inertial forces; Vogel 1996), resuspension and re-distribution of cells during a tidal cycle can be a phenomenon of utmost importance (Mann and Lazier 2006). Adding to that, Stevenson and Peterson (1991) found that emigration into a flow and immigration onto substrata can be important processes that regulate benthic diatom species composition and densities. For example, in a scenario of increased wave height correlated with larger and more frequent flooding of the lower supratidal, the resuspension into the water column of slender epipelic diatoms such as *C. closterium* with its long, narrow "projections" of the frustule might be facilitated, therefore reducing its density in benthic sediment samples. Ubertini et al. (2015) studied erosion thresholds and MPB resuspension in experimentally-modified mud/sand mixtures, and found a direct relationship between chlorophyll-*a* content and resuspension of MPB; thus, the biofilm formed from an inoculum in pure mud resulted in an earlier detachment. Therefore it is reasonable to assume that for unicellular organisms with limited motility, such as the pennate diatom population in the experimental plots, resuspension and horizontal redistribution played a significant role on every tidal flooding.

CONCLUSIONS

To our knowledge, this is the first study that focuses on the recolonization of sedimentary structures in a microbial mat-dominated tidal flat. Besides being novel, our experimental approach was systematic on its sampling, and realistic on its scale (< 1 m), and found that small-size (< 25 μm) raphid pennate diatoms (naviculoids and nitzschioids) drive the colonization process in winter and spring by establishing a critical diatom biomass in a relatively short time, due to their larger biomass in relation to the other colonist, *C. closterium*, and act not only as pioneering species, but they are also present in later stages. Moreover, nitzschioid and naviculoid epipelic diatoms have greater potential for the biostabilization of sediments, and as such they should be considered as keystone species in tidal flats. In the ~ 2 mo surveyed, filamentous cyanobacteria that dominate mature mats did not establish a significant biomass and this is linked to an absence of proper "biological shading" and protection against radiation; thus, the hypothesis that the dominant members of a microbial community can drive the colonization after the physical disruption of the mat is rejected. The dominance of pennate diatoms over other components of the MPB community might lie in extrinsic factors such as the importance of tidal flooding in the re-wetting, resuspension and redistribution of the cells; and intrinsic ones, such as motility, nutrient uptake and high growth rate.

FUNDING

This work was supported by Agencia Nacional de Promoción Científica y Técnica [PICT 2012-309], Consejo Nacional de Investigaciones Científicas y Técnicas [PIP 2013 Nº112] and Secretaría de Ciencia y Técnica-Universidad Nacional del Sur [PGI 24/H138]. JP and CNB were supported by postdoctoral and doctoral fellowships from CONICET, respectively, during part of this research.

REFERENCES

Admiraal W. The ecology of estuarine sediment-inhabiting diatoms. *Prog Phycol Res*, 1984; **3**: 269-322.

Admiraal W, Peletier H, Brouwer T. The seasonal succession patterns of diatom species on an intertidal mudflat: an experimental analysis. *Oikos*, 1984; **42**: 30-40.

Apoya-Horton MD, Yin L, Underwood GJC, Gretz MR. Movement modalities and responses to environmental changes of the mudflat diatom *Cylindrotheca closterium* (Bacillariophyceae). *J Phycol*, 2006; **42**: 379-390.

Barnett A, Méléder V, Blommaert L, Lepetit B, Gaudin P, Vyverman W, Sabbe K, Dupuy C, Lavaud J. Growth form defines physiological photoprotective capacity in intertidal benthic diatoms. *ISME J*, 2015; **9**: 32-45.

Bowler C, Vardi A, Allen AE. Oceanographic and biogeochemical insights from diatom genomes. *Ann Rev Mar Science*, 2010; **2**: 333-365.

Buzzelli E, Gianna R, Marchiori E, Bruno M. Influence of nutrient factors on production of mucilage by *Amphora coffeaeformis* var. *perpusilla*. *Cont Shelf Res*, 1997; **17**: 1171-1180.

Cloern JE, Dufford R. Phytoplankton community ecology: principles applied in San Francisco Bay. *Mar Ecol Prog Ser*, 2005; **285**: 11-28.

Cohen Y, Gurevitz M. The Cyanobacteria –ecology, physiology and molecular genetics. In: Dworkin M, Falkow S, Rosenberg E, Schleifer K-H, Stackebrandt E (eds.). *The Prokaryotes, a handbook on the Biology of Bacteria, Third edition*. New York: Springer, 2006; **4**: 1074-1098.

Consalvey M, Paterson DM, Underwood GJC. The ups and downs of life in a benthic biofilm: migration of benthic diatoms. *Diatom Res*, 2004; **19**: 181-202.

Cuadrado DG, Bournod CN, Pan J, Carmona NB. Microbially-induced sedimentary structures (MISS) as record of storm action in supratidal modern estuarine setting. *Sediment Geol*, 2013; **296**: 1-8.

Cuadrado DG, Carmona NB, Bournod C. Biostabilization of sediments by microbial mats in a temperate siliciclastic tidal flat, Bahía Blanca estuary (Argentina). *Sediment Geol*, 2011; **237**: 95-101.

Cuadrado DG, Perillo GME, Vitale AJ. Modern microbial mats in siliciclastic tidal flats: Evolution, structure and the role of hydrodynamics. *Mar Geol*, 2014; **352**: 367-380.

de Jong L, Admiraal W. Competition between three estuarine benthic diatom species in mixed cultures. *Mar Ecol Prog Ser*, 1984; **18**: 269-275.

de Jonge VN, Colijn F. Dynamics of microphytobenthos biomass in the Ems estuary. *Mar Ecol Prog Ser* 1994; **104**: 185-196.

Decho AW. Microbial exopolymer secretions in ocean environments: their role(s) in food webs and marine processes. *Oceanogr Mar Biol, Ann Rev*, 1990; **28**: 73-153.

Des Marais DJ. Biogeochemistry of hypersaline microbial mats illustrates the dynamics of modern microbial ecosystems and the early evolution of the biosphere. *Biol Bull*, 2003; **204**: 160-167.

Du GY, Li WT, Li H, Chung IK. Migratory responses of benthic diatoms to light and temperature monitored by chlorophyll fluorescence. *J Plant Biol*, 2012; **55**: 159-164.

Edgar LA, Pickett-Heaps JD. Diatom locomotion, an explanation. *Prog Phycol Res*, 1984; **3**: 47-88.

Eppley RW. The growth and culture of diatoms. In: Werner D (ed.). *The biology of diatoms*. Berkeley: University of California Press, 1977, 24-64.

Fernández EM, Spetter CV, Martínez AM, Cuadrado DG, Avena MJ, Marcovecchio JE. Carbohydrate production by microbial mats communities in tidal flat from Bahía Blanca Estuary (Argentina). *Environ Earth Sci*, 2016; **75**: 641.

Gerdes G. Structures left by modern microbial mats in their host sediments. In: Schieber J, Bose PK, Eriksson PG, Banerjee S, Sarkar S, Altermann W, Catuneau O (eds.). *Atlas of microbial mat features preserved within the clastic rock record*. Amsterdam: Elsevier, 2007, 5-38.

Gerdes G, Klenke T, Noffke N. Microbial signatures in peritidal siliciclastic sediments: a catalogue. *Sedimentology*, 2000; **47**: 279-308.

Haubois AG, Sylvestre F, Guarini JM, Richard P, Blanchard GF. Spatio-temporal structure of the epipelic diatom assemblage from an intertidal mudflat in Marennes-Oléron Bay, France. *Estuar Coast Shelf Sci*, 2005; **64**: 385-394.

Hillebrand H, Sommer U. Diversity of benthic microalgae in response to colonization time and eutrophication. *Aquat Bot*, 2000; **67**: 221-236.

Kamp A, de Beer D, Nitsch JL, Lavik G, Stief P. Diatoms respire nitrate to survive dark and anoxic conditions. *Proc Nat Acad Sci USA*, 2011; **108**: 5649-5654.

Kennett DM, Hargraves PE. Benthic diatoms and sulfide fluctuations: upper basin of Pettaquamscutt River, Rhode Island. *Estuar Coast Shelf Sci* 1985; **21**: 577-586.

Kingston MB. Growth and motility of the diatom *Cylindrotheca closterium*: implications for commercial applications. *J N C Acad Sci*, 2009; **125**: 138-142.

Koch EW, Barbier EB, Silliman BR, Reed DJ, Perillo GM, Hacker SD, Granek EF, Primavera JH, Muthiga N, Polasky S, Halpern BS, Kennedy CJ, Kappel CV, Wolanski E. Non-linearity in ecosystem services: temporal and spatial variability in coastal protection. *Front Ecol Environ*, 2009; **7**: 29-37.

Kruschel C, Castenholz RW. The effect of solar UV and visible irradiance on the vertical movements of cyanobacteria in microbial mats of hypersaline waters. *FEMS Microb Ecol*, 1998; **27**: 53-72.

LeGresley M, McDermott G. Counting chamber methods for quantitative phytoplankton analysis: hæmocytometer, Palmer-Maloney cell and Sedgewick-Rafter cell. In: Karlson B, Cusack C, Bresnan E (eds.). *Microscopic and molecular methods for quantitative phytoplankton analysis*. Paris: UNESCO-IOC Manuals and Guides, 2010; **55**: 25-30.

Mann KH, Lazier JRN. *Dynamics of marine ecosystems: biological-physical interactions in the oceans, Third edition*. Oxford: Blackwell Publishing, 2006.

Margulis L, Dolan MF. Life with oxygen. In: *Early Life, Evolution on the Precambrian Earth, Second Edition*. Sudbury, MA: Jones and Bartlett Publishers, 2002, 58-75.

McKew BA, Taylor JD, McGenity TJ, Underwood GJC. Resistance and resilience of benthic biofilm communities from a temperate saltmarsh to desiccation and rewetting. *ISME J*, 2011; **5**: 30-41.

Mitbavkar S, Anil AC. Species interactions within a fouling diatom community: roles of nutrients, initial inoculum and competitive strategies. *Biofouling*, 2007; **23**: 99-112.

Morin S, Vivas-Nogues M, Duong TT, Boudou A, Coste M, Delmas F. Dynamics of benthic diatom colonization in a cadmium/zinc-polluted river (Riou-Mort, France). *Fund Appl Limnol*, 2007; **168**: 179-187.

Noffke N. Multidirected ripple marks rising from biological and sedimentological processes in modern lower supratidal deposits (Mellum Island, southern North Sea). *Geology*, 1998; **26**: 879-882.

Noffke N. Erosional remnants and pockets evolving from biotic-physical interactions in recent lower supratidal environment. *Sediment Geol*, 1999; **123**: 175-181.

Noffke N, Krumbein WE. A quantitative approach to sedimentary surface structures contoured by the interplay of microbial colonization and physical dynamics. *Sedimentology*, 1999; **46**: 417-426.

Odum HT. *Environment, power, and society*. New York: Wiley-Interscience, 1971.

Odum HT. *Systems ecology: an introduction*. New York: Wiley-Interscience, 1983.

Pan J, Bournod CN, Cuadrado DG, Vitale A, Piccolo M.C. Interaction between estuarine microphytobenthos and physical forcings: the role of atmospheric and sedimentary factors. *Int J Geosci*, 2013*a*; **4**: 352-361.

Pan J, Bournod CN, Pizani NV, Cuadrado DG, Carmona NB. Characterization of microbial mats from a siliciclastic tidal flat (Bahía Blanca Estuary, Argentina). *Geomicrob J*, 2013*b*; **30**: 665-674.

Parodi ER, Barría de Cao S. Benthic microalgal communities in the inner part of the Bahía Blanca estuary (Argentina): a preliminary qualitative study. *Oceanol Acta*, 2003; **25**: 279-284.

Paterson DM. Microbial mediation of sediment structure and behavior. In: Stal L, Caumette P (eds.). *Microbial mats; NATO ASI Series, Ser. G: Ecological Sciences*. Berlin: Springer, 1994; **35**: 97-109.

Pizani NV. Valorización de las interacciones microfitobentos-sedimentos en planicies de marea impactadas por el dragado hidráulico. Doctoral Thesis. Universidad Nacional del Sur [in Spanish] 2008.

Pizani NV, Cuadrado DG, Parodi ER. Estudio preliminar de los efectos del dragado sobre aspectos bio-sedimentológicos de las planicies de marea. *Geoacta*, 2006; **31**: 33-39.

Pringle CM, Bowers JA. An *in situ* substratum fertilization technique: diatom colonization on nutrient-enriched, sand substrata. *Can J Fish Aquat Sci*, 1984; **41**: 1247-1251.

Riznyk RZ, Phinney HK. The distribution of intertidal phytopsammon in an Oregon estuary. *Mar Biol*, 1972; **13**: 318-324.

Round FE, Crawford RM, Mann DG. *The diatoms, biology and morphology of the genera*. Cambridge: Cambridge University Press, 1990.

Sauer J, Wenderoth K, Maier UG, Rhiel E. Effects of salinity, light and time on the vertical migration of diatom assemblages. *Diatom Res*, 2002; **17**: 189-203.

Schieber J. Microbial mats in terrigenous clastics: the challenge of identification in the rock record. *Palaios*, 1999; **14**: 3-12.

Scholz B, Liebezeit G. Microphytobenthic dynamics in a Wadden Sea intertidal flat - Part II: Seasonal and spatial variability of non-diatom community components in relation to abiotic parameters. *Eur J Phycol* 2012; **47**: 120-137.

Seuront L, Spilmont N. Self-organized criticality in intertidal microphytobenthos patch patterns. *Physica A*, 2002; **313**: 513-539.

Shepard RN, Sumner DY. Undirected motility of filamentous cyanobacteria produces reticulate mats. *Geobiology*, 2010; **8**: 179-190.

Snoeijs P, Busse S, Potapova M. The importance of diatom cell size in community analysis. *J Phycol*, 2002; **38**: 265-272.

Sommer U. Are marine diatoms favoured by high Si:N ratios? *Mar Ecol Prog Ser*, 1994; **115**: 309-315.

Spetter CV, Buzzi NS, Fernández EM, Cuadrado DG, Marcovecchio JE. Assessment of the physicochemical conditions sediments in a polluted tidal flat colonized by microbial mats in Bahía Blanca Estuary (Argentina). *Marine Poll Bull*, 2015; **91**: 491-505.

Stal LJ. Microphytobenthos as a biogeomorphological force in intertidal sediment stabilization. *Ecol Eng*, 2010; **36**: 236-245.

Stal LJ, van Gemerden H, Krumbein WE. Structure and development of a benthic marine microbial mat. *FEMS Microb Ecol*, 1985; **31**: 111-125.

Stevenson RJ. Effects of current and conditions simulating autogenically changing microhabitats on benthic diatom immigration. *Ecology*, 1983; **64**: 1514-1524.

Stevenson RJ, Peterson CG. Emigration and immigration can be important determinants of benthic diatom assemblages in streams. *Freshwater Biol*, 1991; **26**: 279-294.

Stevenson RJ, Peterson CG, Kirschtel DB, King CC, Tuchman NC. Density-dependent growth, ecological strategies, and effects of nutrients and shading on benthic diatom succession in streams. *J Phycol*, 1991; **27**: 59-69.

Stolz JF. Structure of microbial mats and biofilms. In: Riding RE, Awramik SM (eds.). *Microbial sediments* Springer, Berlin, 2000, 1-8.

Sun J, Liu D. Geometric models for calculating cell biovolume and surface area for phytoplankton. *J Plankton Res*, 2003; **25**: 1331-1346.

Sundbäck K, Enoksson V, Granéli W, Pettersson K. Influence of sublittoral microphytobenthos on the oxygen and nutrient flux between sediment and water: a laboratory continuous-flow study. *Mar Ecol Prog Ser*, 1991; **74**: 263-279.

Tanaka N. The cell division rates of 10 species of attaching diatoms in natural sea water. *Bull Jpn Soc Sci Fish*, 1984; **50**: 969-972.

Thornton DCO, Dong LF, Underwood GJC, Nedwell DB. Factors affecting microphytobenthic biomass, species composition and production in the Colne Estuary (UK). *Aquat Microb Ecol*, 2002; **27**: 285-300.

Ubertini M, Lefebvre S, Rakotomalala C, Orvain F. Impact of sediment grain-size and biofilm age on epipelic microphytobenthos resuspension. *J Exp Mar Biol Ecol*, 2015; **467**: 52-64.

Underwood GJC. Adaptations of tropical marine microphytobenthic assemblages along a gradient of light and nutrient availability in Suva Lagoon, Fiji. *Eur J Phycol*, 2002; **37**: 449-462.

Underwood GJC, Barnett M. What determines species composition in microphytobenthic biofilms? In: Kromkamp JC, de Brouwer JFC, Blanchard GF, Forster RM, Créach V (eds.). *Functioning of microphytobenthos in estuaries*. Amsterdam: Royal Netherlands Academy of Arts and Sciences, 2006, 123-140.

Underwood GJC, Paterson DM. Seasonal changes in diatom biomass, sediment stability and biogenic stabilization in the Severn Estuary. *J Mar Biol Assoc UK*, 1993; **73**: 871-887.

Underwood GJC, Phillips J, Saunders K. Distribution of estuarine benthic diatom species along salinity and nutrient gradients. *Eur J Phycol*, 1998; **33**: 173-183.

Underwood GJC, Provot L. Determining the environmental preferences of four estuarine epipelic diatom taxa: growth across a range of salinity, nitrate and ammonium conditions. *Eur J Phycol*, 2000; **35**: 173-182.

Underwood GJC. Seasonal and spatial variation in epipelic diatom assemblages in the Severn Estuary. *Diatom Res* 1994; **9**: 451-472.

van Gemerden H. Microbial mats: a joint venture. In: Parkes RJ, Westbroek P, de Leeuw JW (eds.). *Marine sediments, burial, pore water chemistry, microbiology and diagenesis*. *Mar Geology*, 1993; **113**: 3-25.

Vogel S. *Life in moving fluids: the physical biology of flow, Second edition*. Princeton, NJ: Princeton University Press, 1996.

Waterbury JB. The Cyanobacteria –isolation, purification and identification. In: Dworkin M, Falkow S, Rosenberg E, Schleifer K-H, Stackebrandt E (eds.). *The Prokaryotes, a handbook on the Biology of Bacteria, Third edition*. New York: Springer, 2006, **4**: 1053-1073.

Webster IT, Ford PW, Hodgson B. Microphytobenthos contribution to nutrient-phytoplankton dynamics in a shallow coastal lagoon. *Estuaries*, 2002; **25**: 540-551.

Whale GF, Walsby AE. Motility of the cyanobacterium *Microcoleus chthonoplastes* in mud. *Brit Phycol J*, 1984; **19**: 117-123.

Williams RB. Division rates of salt marsh diatoms in relation to salinity and cell size. *Ecology*, 1964; **45**: 877-880.

Wolanski E, Brinson MM, Cahoon DR, Perillo GME. Coastal wetlands: a synthesis. In: Perillo GME, Wolanski E, Cahoon DR, Brinson MM (eds.). *Coastal wetlands: an integrated ecosystem approach*. Amsterdam: Elsevier, 2009, 1-62.

Wunsam S, Cattaneo A, Bourassa N. Comparing diatom species, genera and size in biomonitoring: a case study from streams in the Laurentians (Québec, Canada). *Freshwater Biol* 2002; **47**: 325-340.

Zar JH. *Biostatistical analysis, Fourth edition*. Prentice Hall, Upper Saddle River, NJ, 1998.

TABLE AND FIGURE LEGENDS

Table 1. Total cell density (cells cm^{-3}) in controls (n = 2) and experimental plots (n = 6 randomly-distributed points in the plot) at the mid-point and end of the recolonization experiments. Average values ± SE.

winter	**control**	**experimental plot**	one-way ANOVA
Site 1			*p*-value
day 28	243,448 ± 589	1,760,529 ± 237,638	0.0488
day 56	199,828 ± 2,947	4,531,004 ± 596,103	0.0003
Site 3			
day 28	400,835 ± 2,358	3,823,648 ± 482,157	0.0232
day 56	129,092 ± 11,200	4,680,334 ± 622,900	0.0006
spring	**control**	**experimental plot**	one-way ANOVA
Site 1			*p*-value
day 32	140,882 ± 13,558	8,885,169 ± 1,079,790	0.0275
day 56	146,776 ± 11,200	2,177,082 ± 466,023	0.0093
Site 3			
day 25	65,430 ± 589	1,359,694 ± 242,042	0.0493
day 56	125,556 ± 589	2,249,783 ± 387,128	0.0022

Table 2. Biomass ratio between pennate:centric diatoms colonizing experimental plots, as microphytobenthos recolonization of denuded sediment progressed along 56 days. Average values ± SE, based on n = 6 randomly-distributed points in the plot, for each sampling date.

		days after removal of microbial mat													
		0	**3-4**	**7**	**10-11**	**14**	**17-18**	**21**	**24-25**	**28**	**31-32**	**35**	**42**	**49-50**	**56**
winter	Site 1	0.6 ± 0.2	0.5 ± 0.1	2.6 ± 0.7	2.9 ± 1.0	2.2 ± 0.4	1.6 ± 0.5	2.6 ± 0.5	3.4 ± 1.0	3.4 ± 0.9	5.1 ± 1.4	5.8 ± 1.7	4.4 ± 0.7	5.6 ± 2.3	7.4 ± 1.5
	Site 3	4.8 ± 3.8	2.6 ± 0.5	2.8 ± 1.0	4.2 ± 0.9	2.1 ± 0.3	4.4 ± 1.4	3.2 ± 1.3	26.3 ± 22.6	13.4 ± 5.1	4.2 ± 0.6	7.1 ± 1.4	13.7 ± 6.9	12.9 ± 8.1	15.3 ± 4.9
spring	Site 1	2.2 ± 0.8	3.9 ± 2.0	1.2 ± 0.2	4.5 ± 1.1	6.6 ± 2.0	3.0 ± 0.5	3.8 ± 0.7	2.6 ± 0.4	3.7 ± 0.5	22.3 ± 5.9	7.7 ± 2.7	7.2 ± 4.1	4.8 ± 1.9	3.6 ± 1.1
	Site 3	1.6 ± 0.3	2.0 ± 0.6	2.0 ± 0.4	2.0 ± 0.4	2.8 ± 0.7	4.2 ± 1.7	3.0 ± 0.4	7.5 ± 4.6	2.5 ± 0.4	3.2 ± 0.7	4.0 ± 1.1	1.2 ± 0.3	1.3 ± 0.1	4.2 ± 1.0

Figure 1

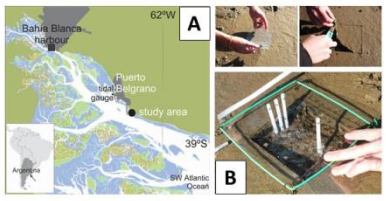

Fig. 1 (**A**) Puerto Rosales (38º 55.5’ S; 62º 03’ W) location within the Bahía Blanca Estuary. (**B**) Photographic sequence of the experiment setup, consisting on removal of a mature microbial mat (~ 2 cm) in a square area of 225 cm^2 to simulate an erosional structure, subdivision of the quadrat into 84 sampling points, and sampling using cylindrical sediment cores (0.385 cm^2 surface area, ~ 0.3 cm height) every 3-4 d for 6 wk, and then every wk for another 2 wk. Note dark, anoxic sediment after mature mat removal.

Figure 2

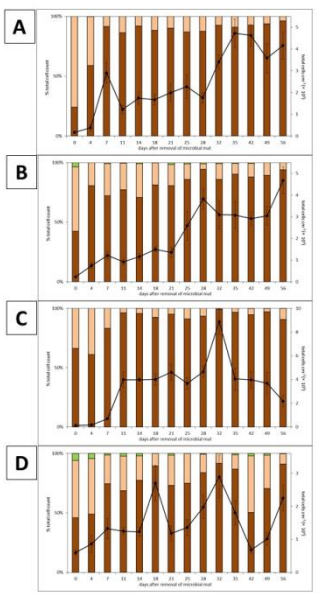

Fig. 2 Patch recolonization experiments in the Bahía Blanca estuary, in Austral winter [(**A**) **S1W** Site 1; and (**B**) **S3W** Site 3: Julian days 151-207]; and Austral spring [(**C**) **S1S** Site 1: Julian days 301-357; and (**D**) **S3S** Site 3: Julian days 280-336]. Bars show the percentage of total cell densities of the most relevant microphytobenthic groups [pennate (brown) and centric diatoms (salmon), filamentous cyanobacteria (green)] in the colonizing biofilm; line represents total cell density (average ± SE; cells cm^{-3}) as the colonization of the patch progresses through time; reference scale plotted in second y axis.

Figure 3

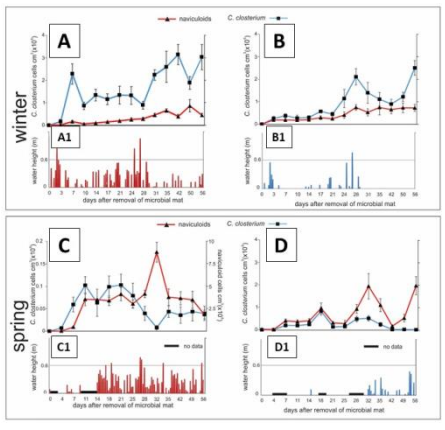

Fig. 3 Dominant pennate diatom populations during patch recolonization experiments in the Bahía Blanca estuary (**A**) **S1W** and (**B**) **S3W**: Julian days 151-207; (**C**) **S1S**: Julian days 301-357; and (**D**) **S3S**: Julian days 280-336. Average cell densities ± SE (cells cm^{-3}) are plotted for *Cylindrotheca closterium* [■], and populations of naviculoid (*Navicula gregaria* and *N. phyllepta*) and nitzschioid (*Nitzschia palea*) pennates [▲], as the colonization of the patch progresses through time. Naviculoid and nitzschioid pennates labelled ‘naviculoids’ in legends for brevity.

Note different y-axis scale for *C. closterium* and naviculoids in **c**. Lower parts of each figure show water column height (m) when supratidal flat gets inundated at: (**A1**) S1W (≥ 3.98 m), and (**B1**) S3W (≥ 4.18 m); (**C1**) S1S; (**D1**) S3S. Black horizontal bars = no data.

Figure 4

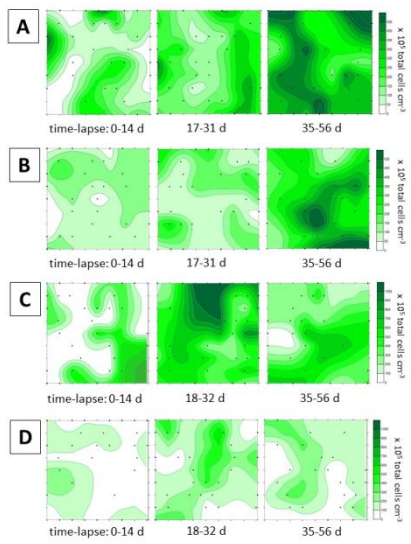

Fig. 4 Two-dimensional density plots summarizing sequential recolonization patterns at three time-intervals after removal of mature microbial mat. (**A**) **S1W**; and (**B**) **S3W**: 0-14 d -left plot-, 17-31 d -center plot-, and 35-56 d -right plot-; (**C**) **S1S**; and (**D**) **S3S**: 0-14 d -left plot-; 18-32 d -center plot-; and 35-56 d -right plot. Dots represent the sampling points in the 225 cm^2 square plot for each time-interval over which density-curves are calculated.

Figure 5

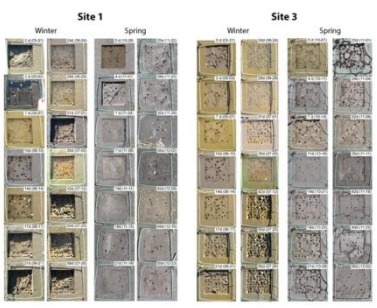

Fig. 5 Photographic sequence of sampling and recolonization of experimental quadrats at Site 1, replicated in Austral winter [(**A**) **S1W** Julian days 151-207] and spring [(**B**) **S1S** Julian days 301-357]; and Site 3, replicated in Austral winter [(**C**) **S3W** Julian days 151-207] and spring [(**D**) **S3S** Julian days 280-336].